CHEMISTRY JOURNAL OF MOLDOVA. General, Industrial and Ecological Chemistry. 2020, 15(1), 21-30
ISSN (p) 1857-1727 ISSN (e) 2345-1688
http://cjm.asm.md
http://dx.doi.org/10.19261/cjm.2019.650

TOWARD A MULTIDISCIPLINARY STRATEGY FOR THE CLASSIFICATION AND REUSE OF IRON AND MANGANESE MINING WASTES

Daniela Guglietta [a], Girolamo Belardi [a], Giovanna Cappai [a,b], Barbara Casentini [c], Alicia Godeas [f], Stefano Milia [a], Daniele Passeri [a], Rosamaria Salvatori [d], Adalgisa Scotti [e], Vanesa Silvani [f], Emanuela Tempesta [a], Stefano Ubaldini [a], Francesca Trapasso [a*]

[a]*Institute of Environmental Geology and Geoengineering, Italian National Research Council, Research Area of Rome 1, 9, Provinciale 35d str., Monterotondo 00015, Italy*
[b]*Department of Civil-Environmental Engineering and Architecture, University of Cagliari, 2, Marengo str., Cagliari 09123, Italy*
[c]*Water Research Institute, Italian National Research Council, Research Area of Rome 1, 9, Provinciale 35d str., Monterotondo 00015, Italy*
[d]*Institute of Atmospheric Pollution Research, Italian National Research Council, Research Area of Rome 1, 9, Provinciale 35d str., Monterotondo 00015, Italy*
[e]*International Center for Earth Sciences, National Atomic Energy Commission, San Rafael M5600, Argentina*
[f]*Faculty of Exact and Natural Science, University of Buenos Aires-CONICET, Institute of Biodiversity, Experimental and Applied Biology, Ciudad Universitaria, 2160, Intendente Guiraldes str., Buenos Aires C1428EGA, Argentina*
[*]*e-mail: francesca.trapasso@igag.cnr.it; phone: (+39 06) 906 72 606; fax: (+39 06) 906 72 733*

Abstract. Mining and mineral-processing wastes have been giving a lot of concern in recent times. This paper has evaluated an integrated multidisciplinary strategy for mining wastes characterization, their possible recycling and reuse, and critical raw materials recovery. After the *in situ* sampling campaigns, mining wastes have been characterized and the acquired mineralogical, chemical and spectral information have been used to create a map of mining waste deposits by means of the new multispectral satellite Sentinel-2A classification. The use of Fe-Mn rich wastes in arsenic removal and phosphorus recovery from water was discussed. Furthermore, mycorrhizal-assisted phytoextraction of metals from contaminated soils classified as Class 1 to 4 by remote sensing showed a good potential for their possible recovery from biomass, and results indicated that the system was suitable for the uptake of several elements. Results are encouraging and the application of such approach can be important to develop a circular model for sustainable exploitation of mining wastes.

Keywords: mining waste, metal recovery, recycle, remote sensing analysis.

Received: 29 October 2019/ Revised final: 02 April 2020/ Accepted: 10 April 2020

Introduction

Resource constraints and environmental pressures are going to accelerate the transformation from a linear extraction-use-throw away model of production and consumption to a circular one. Moving towards a near-zero waste society not only has an environmental rationale, it increasingly becomes a factor of competitiveness. In fact, the technological progress and quality of life are reliant on access to a growing number of raw materials [1]. In this context mining waste not of interest for steel industry because of the low iron content and need of prior ore dressing, can find a valuable use in applications other than mining industry.

Our research has been addressed to mining wastes of one of the largest iron and manganese ore deposits in the State of Odisha (India). In particular, the materials considered not suitable for steel production are dumped in overburden dumps as waste and at the same time, the materials having higher percentage of iron are stored for future use purposes as subgrade. The wastes are particularly rich in iron, manganese and aluminium oxy-hydroxides and represent an important resource because they could be reused as adsorption filters for metals and metalloids, arsenic, as well as in phosphorus removal and recovery from treated wastewater. Iron, aluminium and manganese oxy-hydroxides are

well known adsorbents for the removal of arsenic from waters [2,3]. The possible influence of chemical, spectral and mineralogical properties for a more successful selection of suitable wastes in terms of arsenic removal efficiency has been widely discussed [4]. The potential for recovery and recycling of phosphorus is widely explored in the last decades [5]. On one side, to prevent the load of phosphate present in wastewaters onto surface water bodies with consequent impact on their ecological status [6,7]. On the other side, phosphorus availability as raw materials is critical and different technological solutions to its recovery are now pursued [8-10].

A secondary approach to transform mining wastes into valuable resources is phytoremediation, specifically phyto-mycoremediation, at greatly reduced costs and minimum side effects [11]. Roots of hyperaccumulator plant species establish mutualistic arbuscular mycorrhizal symbiosis with fungi of the phylum *Glomeromycota* [12]. The arbuscular mycorrhizal symbiosis is frequently included in the bioremediation strategies of different metal polluted soils [12-14]. Many studies have demonstrated that the arbuscular mycorrhizal association established between sunflowers (*Helianthus annuus* L.) and the fungus *Rhizophagus intraradices* is effective for the uptake and accumulation of heavy metals [12,13]. Thus, this property could be also used to recover elements from biomass by hydrometallurgical methods.

In the last years, remote sensing technologies have been used to investigate the mining areas finalized to map the spatial distribution of minerals in tailings [15]. However, it is very difficult to have, at the same time, satellite images and mineralogical and geochemical data concerning surface-outcropping materials. It would be important to create synergies between remote sensing and laboratory analysis in order to optimize resources and reduce waste. As a continuation of our research, herein we explore the possibility of classification and reuse of iron and manganese mining wastes to promote the transition to a more circular model of mining wastes sustainable exploration towards near-zero waste, as presented in Figure 1.

The aim of this paper is the identification and classification of mining wastes, the sample collection, analysis and characterization as well as phyto-mycroremediation. Thus, firstly, the capacity of satellite Sentinel-2A is used to classify mining wastes and to identify deposit areas with different percentage of iron and manganese; secondly, the field sampling campaign is conducted to collect mining wastes samples for the laboratory analyses and characterization for the potential reuse for the arsenic removal and phosphorus recovery from water; and lastly, the phyto-mycoremediation of classified mining wastes for raw materials uptake is explored.

Experimental

Samples preparation

During *in situ* sampling campaign, 37 different kinds of samples (rock as well as soil) were collected in the Joda West Iron and Manganese mine, located in village of Joda (Keonjhar district, State of Odisha, India) (Figure 2).

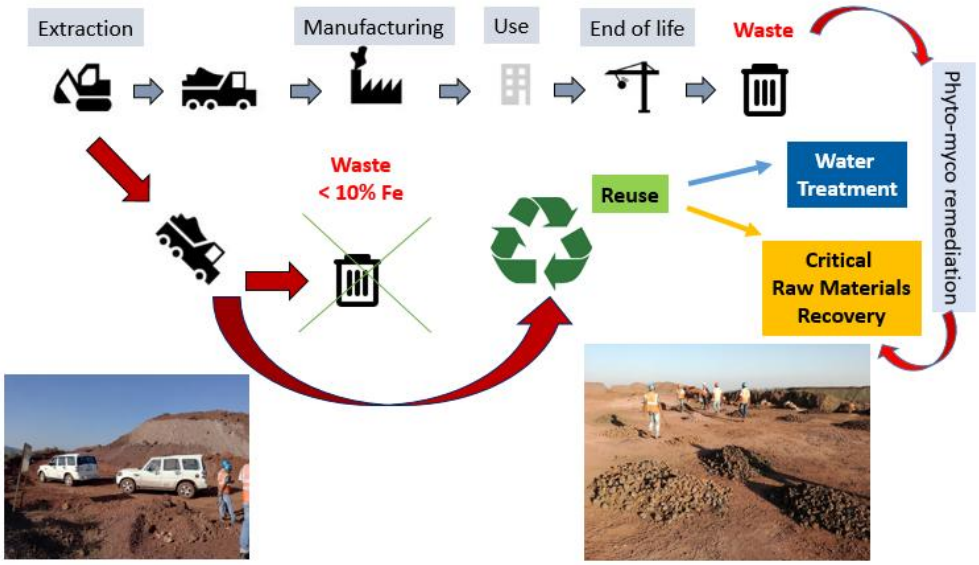

Figure 1. A scheme of the proposed multidisciplinary strategy for classification and reuse of iron and manganese mining wastes.

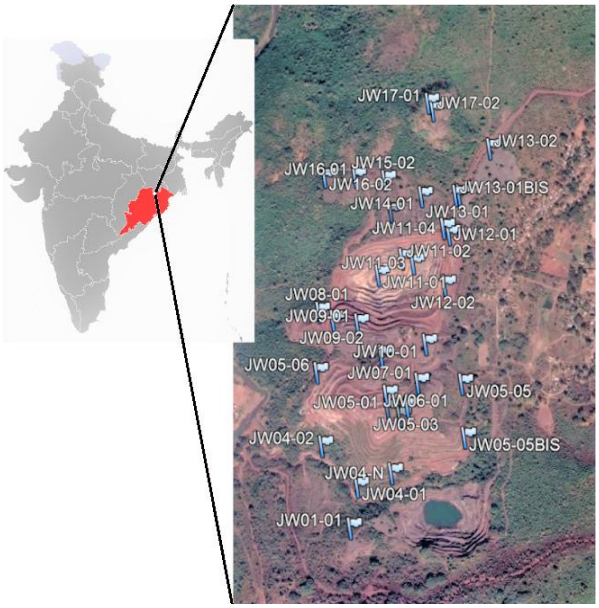

Figure 2. Location of the study area and *in situ* sampling campaign.

From 1933 onward, the mining lease was granted in favour of the TATA Steel, which offered general support during field work performed for this study. For each sample, GPS coordinates, pictures, brief description of the sampling area have been stored. Furthermore, small quantities of samples (for each sample about 200 g) have been selected to further mineralogical and physical analysis at the National Research Council in Italy.

The collected samples were micronized under 70 µ in size by a vibrating rotary cup mill (Willy Bleuler) at 900 rpm motor speed and a standard 100 mL steel crews, and used further in our studies.

Instrumentation

Physical and mineralogical characterization of the soil samples was done by X-ray powder diffraction (XRD) using a Bruker AXS D8 advance diffractometer and X-ray fluorescence (XRF) analysis using the X-ray EDS fluorescence spectrometer (XEPOS HE model).

Arsenic content in solution was determined by atomic absorption spectrometry (AAS, Perkin Elmer AAnalyst 800).

Phosphate content was determined using Hach DR2800 spectrophotometer.

Solution pH was measured using a Hach PHC101 pH-meter connected to a Hach HQ30D digital multiparametric probes reader.

Preliminary evaluation tests of Fe-Mn mining wastes reuse

Arsenic removal and phosphate ions recovery

Five samples, (*JW0504*, *JW1201*, *JW1301bis a*, *JW1301bis b*, and *JW1302*) rich in iron, aluminium and manganese, were selected for evaluation of arsenic removal from the solution.

Batch tests were performed using 50 mg of fine grained (under 70 µ) mining waste materials dispersed in 100 mL MilliQ solution spiked to a level of 1 mg/L As(V) by stock solution of 1 g/L prepared by weighing $Na_2HAsO_4 \cdot 7H_2O$ (Fluka). Samples were collected at time intervals of 0 min, 5 min, 30 min, 60 min, 120 min, 20 hours and 6 days. Samples were mildly shaken at 240 osc/min on a rotatory table throughout the test and filtered onto 0.45 µm cellulose acetate filters, afterwards the content of arsenic in solution was analysed. At the end of the experiment (after 6 days), collected samples were also analysed by inductively coupled plasma mass spectrometry (ICP-MS Agilent 7500c), prior to 0.45 µm filtration and acidification with 2% HNO_3 Suprapur (Merck) to verify possible leaching into water of other potentially toxic metals present in selected materials as evidenced by XRF measurements.

The sample with highest arsenic adsorption capacity was then evaluated for phosphate recovery. A sample portion of 1 g was placed in 50 mL flask containing 40 mL of wastewater solution of 5 mg/L of PO_4^{3-}. The kinetic of phosphate adsorption was evaluated in duplicate at different time intervals 0, 0.5, 1, 2, 4 and 24 hours. Phosphate content was determined by the spectrophotometric method at 882 nm after the formation of a blue molybdenum complex. Batch pH during the adsorption test was maintained constant at 7.0±0.5.

Mycorrhizal assisted phytoremediation

The phyto-mycoremediation system consisted of sunflowers (*Helianthus annuus* L., hybrid cultivar DK4045, Syngenta seeds) colonized by an arbuscular mycorrhizal fungal strain GA5 *Rhizophagus intraradices* (provided *in vitro* by Bank of Glomeromycota, Faculty of Exact and Natural Sciences, Buenos Aires University) grown in a substrate consisting of a homogeneous mixture of soil and volcanic ash (50:50, v/v) supplemented with $ZnSO_4$ (as catalyst).

The soil samples were collected in the Joda West Iron and Manganese mine (Keonjhar district, State of Odisha, India). Volcanic ash was provided by Pumex S.P.A. (Lipari Island, Italy). Granular pumice stone (diameter, 3-6 mm) was provided by Europomice S.R.L. (Italy). Fertile commercial topsoil was provided by Euroterriflora S.R.L. (Italy).

A substrate sample (10 g) was used to detect arbuscular mycorrhizal fungal structures;

it was wet sieved, decanted and checked for arbuscular mycorrhizal fungal spores. Non-indigenous arbuscular mycorrhizal fungal propagules were detected in soil samples. The GA5 strain was propagated as described in Silvani, V.A. *et al.* [16]. The arbuscular mycorrhizal fungus *R. intraradices* strain GA5 has been reported to promote tolerance to different abiotic stresses in several plant species and is a potential bioremediator [17,18].

The experimental design of the TRL 2 system consisted of 16 pots (height, 12 cm; diameter, 13.5 cm), as named and detailed below:

- *CS1-4*$^+$: 4 pots filled with mixed contaminated soil (*CS*) from different areas of the Indian mine and Lipari's volcanic ash (*VA*) in a 1:1 (v/v) ratio, completing to 500 mL and 125 mL granular pumice stone (*PS*; mean diameter, 3-6 mm). Considering the *CS* only, 300-500 ppm $ZnSO_4$ (as catalyst) was added. At least three *Helianthus annuus* seeds were planted and inoculated with a piece of GA5 *in vitro* culture with at least 300 spores in each pot;
- *CS1-4*$^-$: 4 pots filled with mixed *CS* and *VA* in a 1:1 (v/v) ratio, and 125 mL *PS*. Considering the *CS* only, 300-500 ppm $ZnSO_4$ was added. At least three *Helianthus annuus* seeds were planted in each pot;
- *BLS1-4*$^+$: 4 pots filled with 500 mL fertile commercial topsoil (FCT) and 125 mL *PS* by spot. At least three *Helianthus annuus* seeds were planted and inoculated with a piece of GA5 *in vitro* culture with at least 300 spores in each pot;
- *BLS1-4*$^-$: 4 pots filled with 500 mL FCT and 125 mL *PS* by spot. At least three *Helianthus annuus* seeds were planted in each pot.

As to *CS1-4*$^+$ and *CS1-4*$^-$, composition of mixed *CS* from different areas of the Indian mine is reported in Figure 3. Representative soil samples were taken from each pot on days 0 and 133 (*i.e.* the end of the experimental campaign). Samples were dried to constant weight for metals content quantification by the XRF technique.

On day 133, *Helianthus annuus* was removed from each pot, shoots and roots were separated and carefully rinsed with distilled water, dried in an oven (45°C) and analysed by XRF (Wavelength dispersive X-ray fluorescence spectrometer, Panalytical Venus 200), as well as *CS1-4*$^+$, *CS1-4*$^-$, *BLS1-4*$^+$ and *BLS1-4*$^-$. A subsample of roots was stained with trypan blue [19] and intraradical colonization by the arbuscular mycorrhizal fungus GA5 strain was checked. The frequency of mycorrhizal colonization was calculated as the percentage of root segments containing arbuscular mycorrhizal fungal structures. All measurements were performed under a Nikon light binocular microscope at 100x magnification.

The bioconcentration factors (calculated as the ratio between the concentration of metals in the plant tissue and in the soil) in aerial and radicular parts (BC_S and BC_R, respectively), and translocation factors (TF, calculated as the ratio between the concentration of metals in the aerial part and in the roots) were determined for the following metals: As, Ca, Cr, Cu, Fe, Ga, K, Mn, Ni, P, Rb, S, Sr, Ti, Zn.

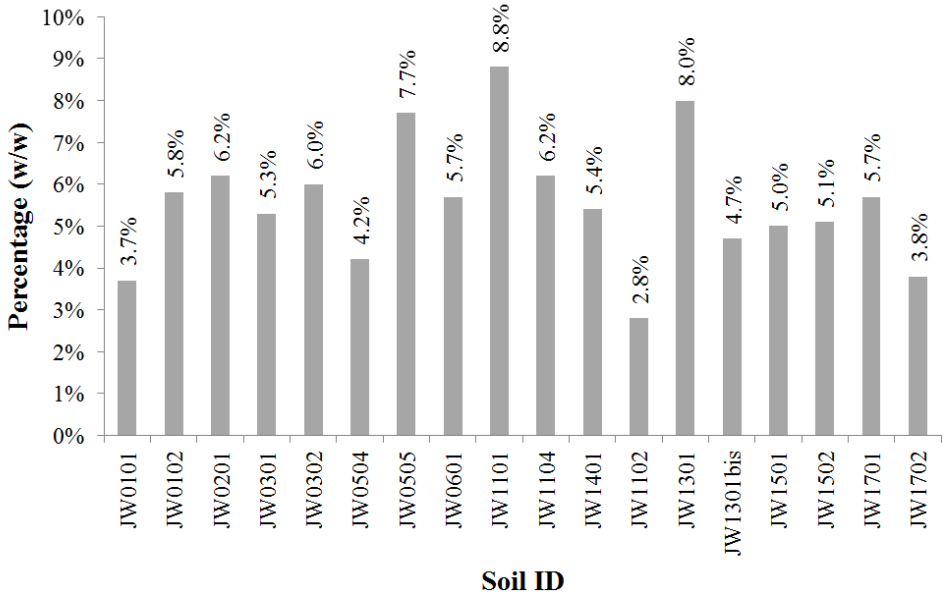

Figure 3. Composition of mixed contaminated soil used to carry out the phyto-mycoremediation experiments.

Results and discussion

Waste mining map by Sentinel-2A satellite

Evaluation of the capability of remote data in characterizing the reflectance of a specific surface is based on their ability in distinguishing one spectrum of specific surface from another, in other words, on their ability in measuring the spectral similarity between one spectrum and another.

In this research, one Sentinel-2A satellite data acquisition was carried out on the iron and manganese mining area on November 29th, 2017 and the sampling sites were recognized on the georeferenced image. For each site, the corresponding spectral signature was extracted by the image and the different spectral classes have been individuated by means of the interpretation of chemical and mineralogical analysis. Afterwards, the map of iron and manganese wastes was obtained through the spectral similarity measurements achieved by the principal supervised classifiers: the classifier used in this methodology was Spectral Angle Mapper (SAM) [20].

The results of SAM classification were represented in an iron and manganese waste mining map that highlights waste deposit areas with different mean percentage of iron and manganese (Figure 4).

In particular, the presence of vegetation in Class 1 indicates that the wastes have been accumulated over an extended period compared to Class 2, characterized by a steady accumulation of extractive wastes. Class 3 is very rich in iron and manganese but these deposits of residues are not of interest for steel industry and need prior ore dressing. Finally, in Class 4 there are wastes with lower iron and manganese content.

Image accuracy was computed matching the ground truth classes with the classification result classes. The accuracy of the classification, derived from the confusion matrix, resulted as follows:

- user's accuracy = 94.81%;
- producer's accuracy = 95.23%;
- overall accuracy = 95.88%; k= 0.806.

These results point out the capacity of Sentinel-2A to classify mining wastes but also to identify deposits with valuable materials in order to reuse for secondary applications. In particular, the deposit areas of residues rich in iron and manganese represent the potential site for further analysis (*i.e.* arsenic removal and phyto-mycoremediation application).

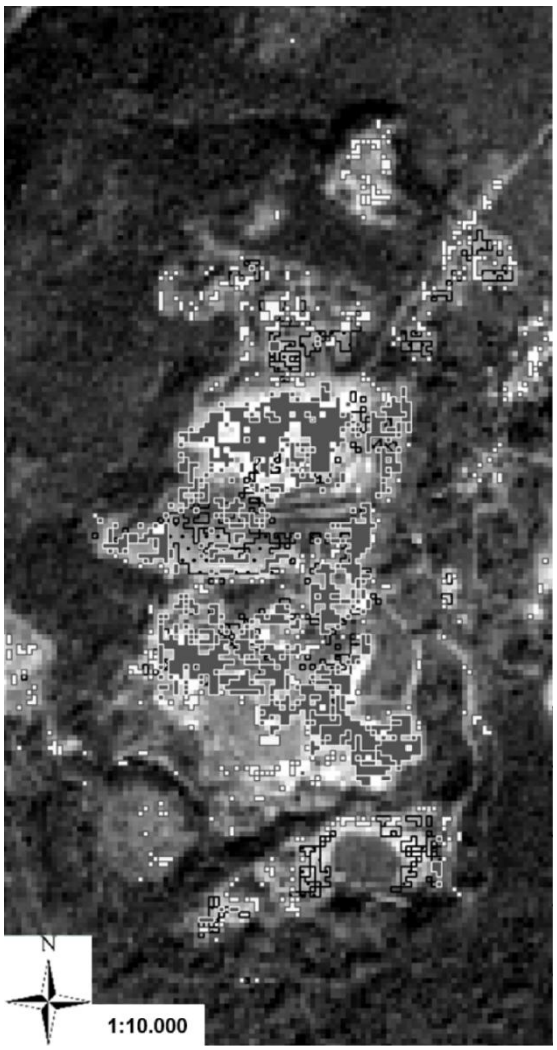

	Fe mean (%)	Mn mean (%)
Class 1	37.99	13.18
Class 2	40.34	9.6
Class 3	42.44	18.2
Class 4	22.86	1.3

Figure 4. Iron and manganese mining wastes deposits map. The four classes have been overlaid on Sentinel-2A image of the location map.

Arsenic removal efficiency

A selection of five samples was carried out among all characterized samples, based on iron, manganese and aluminium content and major mineralogical phases (Tables 1 and 2).

Among all iron oxides minerals (magnetite, lepidocrocite, maghemite, goethite, ferrihydrite, and hematite), according to XRD results (Table 1) the mostly present were iron hydroxides phases including hematite and goethite, while sample *JW0504* was selected due to its high percentage of aluminium (52.5% kaolinite). Manganese content was up to 46.9% in sample *JW1301bis b*. It should be observed that in these samples the presence of potentially toxic metals, including arsenic, was not always negligible. Chromium content was almost 400 mg/kg and lead about 300 mg/kg in sample *JW0504*. Preliminary kinetic batch adsorption tests were conducted to evaluate the efficiency in As(V) removal by selected waste materials (Figure 5).

At selected solid/water ratio (0.5 g/L), arsenic adsorption was below 30% for all samples during the first 30 min, increasing up to 41% and 53% for sample *JW0504* and *JW1301bis a*, respectively, after 6 days of contact time. Among iron hydroxides, the presence of goethite seems to promote the adsorption. If compared to commercially available materials the adsorption kinetic of these waste materials is not fast, since usually iron oxy-hydroxide used in As removal filters, such as granular ferric hydroxide (GFH) that was used in this study, are able to remove up to 90% As within first 5 min (contact time usually used in water filtration unit). Banerjee, D. *et al*. [21] found that at lower As(V) concentration (0.1 mg/L) a solution with 0.25 adsorbent to liquid ratio was able to completely remove As(V) within 2 hours. In this study, the ability of some selected materials to adsorb 30-50% of arsenic is interesting since these wastes are low cost materials largely available at Joda mining site and the efficiency in removal could be easily increased by increasing filter volume and adsorbent amount. The adsorption capacity of the studied samples ranged from 0.41 to 1.0 mg/g (As/adsorbent), while GFH had a capacity of 1.94 mg/g (As/adsorbent). Naturally occurring iron-rich materials usually show lower adsorption capacity than synthetic oxides and iron rich ore materials tested by Zhang, W. *et al*. [22], which had a maximum adsorption capacity of 0.17-0.48 mg/g (As/adsorbent).

A possible release of potentially toxic elements in solution was investigated after 6 days and results are reported in Table 3. The mobility of other toxic metals in these samples resulted to be limited and concentrations values are far below drinking water limits (EU Directive 98/83: Cr 50 μg/L, Cu 1 mg/L and Zn are not regulated).

Table 1

Selected samples for adsorption tests, their major metals content and the dominant mineralogical components (in %).

Sample Code	*Fe*	*Al*	*Mn*	*Hematite*	*Goethite*	*Muscovite*	*Kaolinite*	*Pyrolusite*
JW1201	39.1	3.6	15.6	36.9	2.4	n.d.	22.2	n.d.
JW1301bis b	16.9	1.3	46.9	19.8	6	19.8	18.1	10.8
JW1302	28.5	2	29.1	10.8	6.7	26.1	16.8	6.3
JW0504	9.8	13.8	1.8	4.4	4.2	20.3	52.5	n.d.
JW1301bis a	49.5	3.2	1.8	23.4	25.4	20.1	15.3	n.d.

n.d. = not detectable phases

Table 2

Selected samples for adsorption tests and their trace metals content (in mg/kg).

Sample Code	*As*	*Cr*	*Cu*	*Ni*	*Pb*	*Zn*
JW1201	n.d.	17.6	35.2	41.5	44	53.5
JW1301bis b	n.d.	53.1	95.6	48.2	130	48.9
JW1302	n.d.	60.7	128.6	107.6	37	92.6
JW0504	20.5	387.3	49.4	79.4	309.5	28.9
JW1301bis a	64.7	193.4	42.3	40.8	2.8	53.7

n.d. = not detectable phases

Table 3

Release into water of potentially toxic metals after 6 days contact. (Concentration is expressed as μg/L)

Sample Code	*V*	*Cr*	*Cu*	*Zn*	*Cd*	*Pb*	*U*
JW1201	< 0.05	0.11	0.07	16.3	< 0.05	< 0.05	< 0.05
JW1301bis b	< 0.05	0.29	0.08	5.6	< 0.05	< 0.05	< 0.05
JW1302	0.07	0.14	0.06	2.0	< 0.05	< 0.05	< 0.05
JW0504	0.71	0.65	0.06	1.8	< 0.05	< 0.05	< 0.05
JW1301bis a	< 0.05	0.55	0.12	11.3	< 0.05	< 0.05	< 0.05

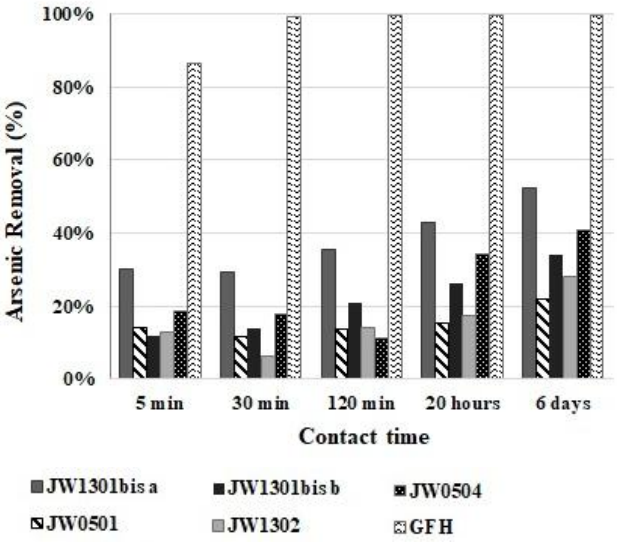

Figure 5. Batch kinetic study of As(V) removal (%) for 5 different samples (0.5 g/L) and the commercial granular ferric oxide (GFH).
Initial As(V) concentration was 1 mg/L.

Phosphate removal/recovery capacity

Sample *JW1301bis a* has shown the highest arsenic removal capacity and was further used to test also the ability to recover phosphate from a wastewater solution containing 5 mg/L of phosphate. Initial phosphate content was reduced by 95% within 30 min (Figure 6).

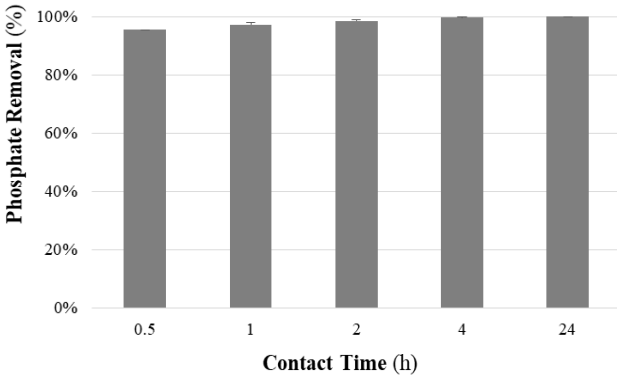

Figure 6. Phosphate removal (mean and standard deviation reported) using the sample *JW1301bis a*.

Final adsorption capacity was about 0.065 mg/g of phosphorus (the mass ratio of phosphate ions to phosphorus was 94.97/30.97 or 3.066 to 1) under neutral condition (pH= 7±0.5). Huang, W.W. *et al.* [23] tested the ability of red mud for phosphorus recovery in 1 mg/L effluent. They reported a plateau for removal after 5 hours with increasing adsorbing capacity up to 0.4 mg/g of phosphorus under acidic condition.

Phyto-mycoremediation of contaminated soil by Helianthus annuus and Rhizophagus intraradices

The concentration of elements in pots containing blank (*BLS*) and contaminated soils (*CS*), in volcanic ash (*VA*) and in granular pumice stone (*PS*) is reported in Table 1S (Supplementary material).

CS values correspond to areas classified as Class 4 by remote sensing (Figure 4) by their content (%) of Mn and Fe, 5.07±0.21 and 14.7±0.4, respectively. Although the sample extraction points correspond to areas classified by remote sensing as Class 1 and 2, the mixed proportion of the amounts of soil in each region (shown in Figure 3) and the addition of volcanic ash caused a dilution effect. *CS* values shown in Table 1S (from Supplementary material) present relevant amounts of CRMs as Ga (12.4±0.6 ppm), as well as of raw materials like Zn (1315.2±53.2 ppm), which encourage their possible recovery. Moreover, high concentrations of contaminants such as Cr (131.0±2.7 ppm) and As (11.9±0.2 ppm) are reported.

No significant difference in plant growth (*i.e.*, leaves development and length of the aerial parts) was observed among pots filled with the contaminated and the blank soils. Therefore, the presence of high contamination levels (especially of Mn and Fe) did not influence the development of *Helianthus annuus* plants. Moreover, no differences were found between mycorrhized and non-mycorrhized plants, indicating that the presence of *Rhizophagus intraradices* in roots did not influence plant growth development.

The arbuscular mycorrhizal fungus *Rhizophagus intraradices* strain GA5 colonized sunflower roots at 5±4.4% and 42±5.4% in the CS^+ and BLS^+ treatments, respectively. Typical arbuscular mycorrhizal fungal structures were observed in sunflower roots with abundant vesicles and hyphae (Figure 7*(a)*). As expected, no arbuscular mycorrhizal root colonization was observed in the BLS^- and CS^- treatments (Figure 7*(b)*).

Table 2S (Supplementary material) reports the average concentration of elements in $CS1\text{-}4^+$ and $CS1\text{-}4^-$, as well as in related biomass (shoots and roots) after the phyto-mycoremediation treatment. Preliminary results indicated that the system was suitable for the uptake of some elements: Mn, Fe, Zn, P, Cr, Cu, Ga and As. A similar result was also found by Rivelli, A.R. *et al*. [24] for uptake of Zn, Cd and Cu, and for Mn by Hajiboland, R. *et al*. [25].

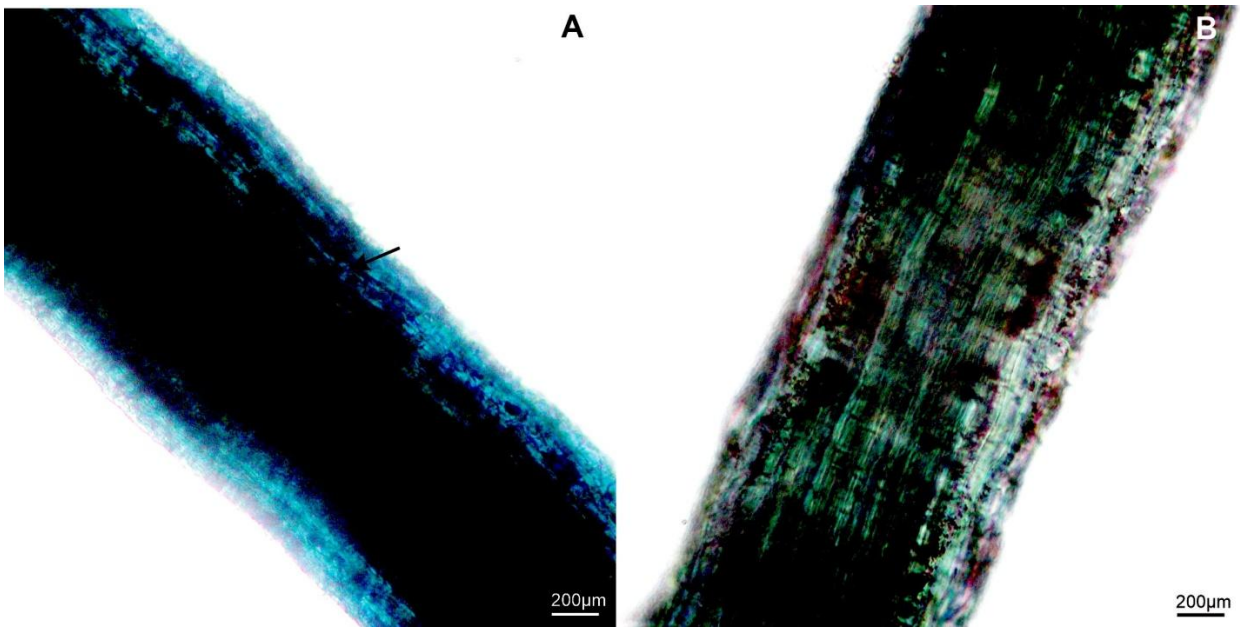

(a) ***(b)***

Figure 7. Root colonization of sunflower plant by the arbuscular mycorrhizal fungus *Rhizophagus intraradices* GA5 strain after 133 days.
***(a)* Detail of sunflower roots with intraradical hyphae, arbuscules and vesicles developed by the arbuscular mycorrhizal fungus are indicated by the arrow.**
***(b)* Uncolonized root of sunflower plant in control treatment.**

Table 4

Bioconcentration and translocation factors measured in *CS1-4*$^+$ and *CS1-4*$^-$.

	As	*Ca*	*Cr*	*Cu*	*Fe*	*Ga*	*K*	*Mn*	*P*	*Ni*	*Rb*	*S*	*Sr*	*Ti*	*Zn*
BC_S^+	0.17	2.14	0.02	0.26	0.00	1.57	3.50	0.01	5.35	0.02	1.44	5.28	3.65	0.01	0.90
BC_S^-	0.12	1.84	0.01	0.23	0.00	1.06	3.09	0.01	3.94	0.01	1.30	5.18	2.31	0.01	0.94
BC_R^+	0.28	0.94	0.26	0.27	0.10	1.27	2.11	0.08	1.73	0.53	0.16	15.01	0.70	0.17	0.79
BC_R^-	0.52	2.19	0.09	0.60	0.19	1.71	2.28	0.15	1.20	0.21	1.39	11.53	1.26	0.37	1.14
TF^+	0.62	2.28	0.09	0.94	0.02	1.23	1.66	0.11	3.10	0.05	9.28	0.35	5.19	0.02	1.14
TF^-	0.23	0.84	0.07	0.39	0.01	0.62	1.35	0.07	3.27	0.07	0.94	0.45	1.84	0.02	0.82

The mycorrhizal colonization enhanced the uptake of Cr, P and Ni in sunflower shoots and roots, of As, Ga and Sr in shoots, while S uptake was enhanced only in sunflower roots. Conversely, the uptake of Ca, Cu, Mn, Rb, Sr, Ti and Zn was reduced in mycorrhized sunflower roots, indicating that mycorrhizal fungus *Rhizophagus intraradices* GA5 strain did not have an univocal effect on elements accumulation in biomass.

Table 4 reports the accumulation coefficients measured at the end of the experimental period. As to mycorrhized systems *CS1-4*$^+$, bioconcentration factors in shoots (BC_S^+) followed the order: P(5.35)>S>Sr>K>Ca>Ga>Rb >Zn(0.9)>Cu>As>Ni>Cr>Mn(0.01)>Ti=Fe(0.00); bioconcentration factors in roots (BC_R^+) followed the order: S(15.01)>K>P>Ga>Ca(0.94)>Zn>Sr> Ni>As>Cu>Cr>Ti>Rb>Fe(0.10)>Mn(0.08); the translocation factor followed the order: Rb(9.28)>Sr>P>Ca>K>Ga>Zn>Cu(0.94)>As>S> Mn>Cr>Ni (0.05)>Fe=Ti(0.02).

As to biomass in *CS1-4*$^-$, bioconcentration factors in shoots (BC_S^-) followed the order: S(5.2)>P>K>Sr>Ca>Rb>Ga(1.06)>Zn(0.94)>Cu >As>Ni>Mn>Ti>Cr>Fe(0.003); bioconcentration factors in roots (BC_R^-) followed the order: S(11.53)>K>Ca>Ga>Rb>Sr>P>Zn(1.14)>Cu>As >Ti>Ni>Fe>Mn>Cr(0.09); the translocation factor followed the order: P(3.3)>Sr>K>Rb(0.94)>Ca>Zn>Ga>S>Cu>As> Mn>Ni>Cr>Ti>Fe (0.01).

It should be considered that the observed values of BC_S and BC_R for Mn and Fe are low due to the very high concentration of such elements in soil, rather than to a poor bioconcentration potential: in fact, low *BC* values coexisted with high concentrations of

Mn and Fe in biomass (Table 2S from Supplementary material).

Despite such promising results, it must be noticed that the overall biomass growth was not sufficient to sustain a significant recovery of elements at this stage (for instance by hydrometallurgical methods), therefore process conditions must be optimized in order to maximise biomass growth.

Conclusions

This methodology explores the advantage to employ an integrated approach to characterize and map as well as reuse mining wastes. The preliminary encouraging results highlight that the application of this approach is very useful and important to develop a circular model for sustainable exploitation of mining wastes towards near-zero waste.

The multispectral sensor such as MSI (MultiSpectral Imager) on Sentinel-2A provides the cheapest images that can be used for mineral land characterization. The resulting remotely mining waste mapping constitutes a valuable tool for optimizing *in situ* sampling strategies aimed at selecting more suitable mining waste to be reused.

Preliminary tests encourage further studies on the possible application of mining waste materials in water treatment, both for arsenic removal and phosphate removal/recovery. Arsenic removal was in the range of 40-60% and the efficiency could be enhanced by increasing the amount of solid material used to realize a filter. Phosphate adsorption was above 90%, therefore waste materials could also be successfully used to reduce phosphate load into surface water. Furthermore, in order to increase adsorption properties, mineralogical enrichment processes of higher adsorptive selected Fe minerals phases can be adopted. The possible release of toxic metals from these materials has been found negligible according to EU drinking water regulations.

As to phyto-mycoremediation tests, preliminary results show that it is possible to obtain the growth of the phyto-mycoremediation system in areas classified by remote sensing as Class 1, 2, 3 and 4. The observed bioconcentration factors and translocation factors values (>0.9-1.0), or the high concentration of certain elements in biomass, proved that such system was effective for the phytostabilization or phytoextraction of Fe, Mn, P, Rb, Ga, Cu, S, Sr, and Zn, although the experimental conditions should be optimized in order to obtain sufficient biomass quantities for metals recovery through hydrometallurgical methods.

Acknowledgments

This research was supported by Teco project. The authors are grateful to the staff of TATA Steel for providing general support during field work.

Supplementary information

Supplementary data are available free of charge at http://cjm.asm.md as PDF file.

References

1. Ubaldini, S.; Guglietta, D.; Trapasso, F.; Carloni, S.; Passeri, D.; Scotti, A. Treatment of secondary raw materials by innovative processes. Chemistry Journal of Moldova, 2019, 14(1), pp. 32-46. DOI: http://dx.doi.org/10.19261/cjm.2019.585
2. Mohan, D.; Pittman Jr., C.U. Arsenic removal from water/wastewater using adsorbents-A critical review. Journal of Hazardous Materials, 2007, 142, pp. 1-53. DOI: https://doi.org/10.1016/j.jhazmat.2007.01.006
3. Jeong, Y.; Fan, M.; Singh, S.; Chuang, C.L.; Saha, B.; van Leeuwen, J.H. Evaluation of iron oxide and aluminum oxide as potential arsenic(V) adsorbents. Chemical Engineering and Processing-Process Intensification, 2007, 46(10), pp. 1030-1039. DOI: https://doi.org/10.1016/j.cep.2007.05.004
4. Casentini, B.; Lazzazzara, M.; Amalfitano, S.; Salvatori, R.; Guglietta, D.; Passeri, D.; Belardi, G.; Trapasso, F. Mining rock wastes for water treatment: potential reuse of Fe- and Mn-rich materials for arsenic removal. Water, 2019, 11(9), pp. 1897. DOI: https://doi.org/10.3390/w11091897
5. Cordell, D.; Rosemarin, A.; Schroeder, J.J.; Smit, A.L. Towards global phosphorus security: A systems framework for phosphorus recovery and reuse options. Chemosphere, 2011, 84(6), pp. 747-758. DOI: https://doi.org/10.1016/j.chemosphere.2011.02.032
6. Carpenter, S.R.; Caraco, N.F.; Correll, D.L.; Howarth, R.W.; Sharpley, A.N.; Smith, V.H. Nonpoint pollution of surface waters with phosphorus and nitrogen. Ecological Applications, 1998, 8(3), pp. 559-568. DOI: https://doi.org/10.1890/1051-0761(1998)008[0559:NPOSWW]2.0.CO;2
7. Jarvie, H.P.; Neal, C.; Withers, P.J.A. Sewage-effluent phosphorus: a greater risk to river eutrophication than agricultural phosphorus? Science of the Total Environment, 2006, 360(1-3), pp. 246-253. DOI: https://doi.org/10.1016/j.scitotenv.2005.08.038
8. Pan, B.; Wu, J.; Pan, B.; Lv, L.; Zhang, W.; Xiao, L.; Wang, X.; Tao, X.; Zheng, S. Development of polymer-based nanosized hydrated ferric oxides (HFOs) for enhanced phosphate removal from waste effluents. Water Research, 2009, 43(17), pp. 4421-4429.

DOI: https://doi.org/10.1016/j.watres.2009.06.055
9. Blaney, L.M.; Cinar, S.; SenGupta, A.K. Hybrid anion exchanger for trace phosphate removal from water and wastewater. Water Research, 2007, 41(7), pp. 1603-1613. DOI: https://doi.org/10.1016/j.watres.2007.01.008
10. Yan, L.G; Xu, Y.Y.; Yu, H.Q.; Xin, X.D.; Wei, Q.; Du, B. Adsorption of phosphate from aqueous solution by hydroxy-aluminum, hydroxy-iron and hydroxy-iron–aluminum pillared bentonites. Journal of Hazardous Materials, 2010, 179(1-3), pp. 244-250. DOI: https://doi.org/10.1016/j.jhazmat.2010.02.086
11. Glick, B.R. Phytoremediation: synergistic use of plants and bacteria to clean up the environment. Biotechnology Advances, 2003, 21(5), pp. 383-393. DOI: https://doi.org/10.1016/S0734-9750(03)00055-7
12. Smith, S.E.; Read, D.J. Mycorrhizal Symbiosis. 3rd Edition, Academic Press: London, 2008, 800 p. https://www.elsevier.com/books/mycorrhizal-symbiosis/smith/978-0-12-370526-6
13. Ker, K; Charest, C. Nickel remediation by AM-colonized sunflower. Mycorrhiza, 2010, 20, pp. 399-406. DOI: https://doi.org/10.1007/s00572-009-0293-7
14. Yang, Y.; Liang, Y.; Han, X.; Chiu, T.Y.; Ghosh, A.; Chen, H.; Tang, M. The roles of arbuscular mycorrhizal fungi (AMF) in phytoremediation and tree-herb interactions in Pb contaminated soil. Scientific Reports, 2016, 6, pp. 20469. DOI: https://doi.org/10.1038/srep20469
15. Zabcic, N.; Rivard, B.; Ong, C.; Mueller, A. Using airborne hyperspectral data to characterize the surface pH and mineralogy of pyrite mine tailings. International Journal of Applied Earth Observation and Geoinformation, 2014, 32, pp. 152-162. DOI: https://doi.org/10.1016/j.jag.2014.04.008
16. Silvani, V.A.; Bidondo, L.F.; Bompadre, M.J.; Colombo, R.P.; Pérgola, M.; Bompadre, A.; Fracchia, S.; Godeas, A. Growth dynamics of geographically different arbuscular mycorrhizal fungal isolates belonging to the 'Rhizophagus clade' under monoxenic conditions. Mycologia, 2014, 106(5), pp. 963-975. DOI: https://doi.org/10.3852/13-118
17. Bompadre, M.J.; Silvani, V.A.; Bidondo, L.F.; Ríos de Molina, M.C.; Colombo, R.P.; Pardo, A.G.; Godeas, A.M. Arbuscular mycorrhizal fungi alleviate oxidative stress in pomegranate plants growing under different irrigation conditions. Botany, 2014, 92(3), pp. 187-193. DOI: https://doi.org/10.1139/cjb-2013-0169
18. Scotti, A.; Silvani, V.A.; Cerioni, J.; Visciglia, M.; Benavidez, M.; Godeas A. Pilot testing of a bioremediation system for water and soils contaminated with heavy metals: vegetable depuration module. International Journal of Phytoremediation, 2019, 21(9), pp. 899-907. DOI: https://doi.org/10.1080/15226514.2019.1583634
19. Phillips, J.M.; Hayman, D.S. Improved procedures for clearing roots and staining parasitic and vesicular-arbuscular mycorrhizal fungi for rapid assessment of infection. Transactions of the British Mycological Society, 1970, 55(1), pp. 158-161. DOI: https://doi.org/10.1016/S0007-1536(70)80110-3
20. Kruse, F.A.; Lefkoff, A.B.; Boardman, J.W.; Heidebrecht, K.B.; Shapiro, A.T.; Barloon, P.J.; Goetz, A.F.H. The spectral image processing system (SIPS) - Interactive visualization and analysis of imaging spectrometer data. Remote Sensing of Environment, 1993, 44(2-3), pp. 145-163. DOI: https://doi.org/10.1016/0034-4257(93)90013-N
21. Banerjee, D.; Lelandais, G.; Shukla, S.; Mukhopadhyay, G.; Jacq, C.; Devaux, F.; Prasad, R. Responses of pathogenic and nonpathogenic yeast species to steroids reveal the functioning and evolution of multidrug resistance transcriptional networks. Eukaryotic cell, 2008, 7(1), pp. 68-77. DOI: https://doi.org/10.1128/EC.00256-07
22. Zhang, W.; Singh, P.; Paling, E.; Delides, S. Arsenic removal from contaminated water by natural iron ores. Minerals Engineering, 2004, 17(4), pp. 517-524. DOI: https://doi.org/10.1016/j.mineng.2003.11.020
23. Huang, W.; Wang, S.; Zhu, Z.; Li, L.; Yao, X.; Rudolph, V.; Haghseresht, F. Phosphate removal from wastewater using red mud. Journal of Hazardous Materials, 2008, 158(1), pp. 35-42. DOI: https://doi.org/10.1016/j.jhazmat.2008.01.061
24. Rivelli, A.R.; De Maria, S.; Puschenreiter, M.; Gherbin, P. Accumulation of cadmium, zinc, and copper by *Helianthus Annuus L.*: impact on plant growth and uptake of nutritional elements. International Journal of Phytoremediation, 2012, 14(4), pp. 320-334. DOI: https://doi.org/10.1080/15226514.2011.620649
25. Hajiboland, R.; Aliasgharpour, M.; Dashtbani, F.; Movafeghi, A.; Dadpour, M.R. Localization and study of histochemical effects of excess Mn in Sunflower (*Helianthus annuus* L. cv. Azarghol) plants. Journal of Sciences, Islamic Republic of Iran, 2008, 19(4), pp. 305-315. https://jsciences.ut.ac.ir/article_31902.html